Geophysical Research Letters

RESEARCH LETTER
10.1029/2024GL113165

# Absence of Elevation-Dependent Warming in Antarctica Inferred From Blue Ice Paleoclimate Records

**Etienne Legrain[1,2], Veronica Tollenaar[1,2], Steven Goderis[3], Lisa Ardoin[1], Pierre-Henri Blard[1,4], Philippe Claeys[3], Raúl R. Cordero[5], Vinciane Debaille[6], François Fripiat[1], Philippe Huybrechts[7], Naoya Imae[8,9], Maaike Izeboud[2], Frank Pattyn[1], Hamed Pourkhorsandi[10,11], Julien Seguinot[2], Naoki Shirai[12,13], Marijke Vancappellen[2], Matthias Van Ginneken[14], Sarah Wauthy[1], Akira Yamaguchi[8,9], Mehmet Yesiltas[15], and Harry Zekollari[1,2,16]**

[1]Laboratoire de Glaciologie, Université libre de Bruxelles, Brussels, Belgium, [2]Department of Water and Climate, Vrije Universiteit Brussel, Brussels, Belgium, [3]Archaeology, Environmental Changes and Geo-Chemistry, Vrije Universiteit Brussel, Brussels, Belgium, [4]CRPG, CNRS, Université de Lorraine, Nancy, France, [5]Universidad de Santiago de Chile, Santiago, Chile, [6]Laboratoire G-Time, Université libre de Bruxelles, Brussels, Belgium, [7]Earth System Science & Departement Geografie, Vrije Universiteit Brussel, Brussels, Belgium, [8]National Institute of Polar Research, Tachikawa, Japan, [9]The Graduate University for Advanced Studies, Hayama, Japan, [10]Laboratoire G-Time, Department of Geosciences, Environment and Society, Université libre de Bruxelles, Brussels, Belgium, [11]Géosciences Environnement Toulouse (GET), IRD/CNRS/UPS/CNES, OMP, Toulouse, France, [12]Department of Chemistry, Graduate School of Science, Tokyo Metropolitan University, Hachioji, Japan, [13]Faculty of Science, Kanagawa University, Yokohama, Japan, [14]Centre for Astrophysics and Planetary Science, School of Physical Sciences, University of Kent, Canterbury, UK, [15]Department of Geosciences, Stony Brook University, Stony Brook, NY, USA, [16]Laboratory of Hydraulics, Hydrology and Glaciology (VAW), ETH Zürich, Zurich, Switzerland

**Abstract** Reconstructing the past Antarctic climate commonly involves deep drilling of ice cores. However, the ∼1% of the Antarctic ice sheet surface covered with blue ice also provides unique, yet largely unexploited paleoclimatic opportunities. Here, we analyze 444 ice samples collected in blue ice surfaces located around the Sør Rondane Mountains. Isotope measurements ($\delta^{18}O$) on these samples enable us to estimate surface paleotemperatures for both the current interglacial period and the Last Glacial Maximum. Combining these paleotemperatures with the spatially varying source elevation of the sampled blue ice provides new insights on the (lack of) lapse rate evolution (i.e., changes in the elevation-temperature relationship) outside the 40°N–40°S latitudinal band. This result contrasts with low-latitude areas that have experienced elevation-dependent warming (EDW) during this period. Our results hint at a future (lack of) EDW in Antarctica, thereby highlighting the potential of blue ice area paleoclimatic archives to better predict future climatic changes.

**Plain Language Summary** Accessing past climatic information in Antarctica typically involves deep vertical ice drilling, a time-consuming, expensive, and technically challenging process. Here, we present a complementary method by sampling surface ice from the blue ice areas (BIA) that cover ∼1% of the total ice sheet area. This blue ice, originating from deeper layers within the ice sheet, emerges at the surface due to local climatic conditions, bedrock topography, and an upward ice flow. In this study, we sampled blue ice in and around a mountain range located in East Antarctica. By analyzing the isotopic composition of the ice, we infer surface temperatures during past warm and cold periods. We find a similar relationship between temperature and elevation across both cold and warm periods. Our finding that warming events are not amplified at high elevations in this region of Antarctica contrasts with previous studies that show the existence of elevation-dependent warming at lower latitude regions. As such, our study highlights that BIAs are a unique asset for constraining potential future high-elevation climatic conditions over the Antarctic ice sheet.

**Key Points:**

- Analyses of surface Antarctic blue ice offer a reconstruction of temperature changes at different elevations during the last deglaciation
- This study presents the first reconstruction of lapse rate evolution during the last deglaciation beyond the 40°N–40°S latitudinal band
- No elevation-dependent warming (i.e., lapse rates remain constant) is registered in Antarctica during the last deglaciation

**Supporting Information:**

Supporting Information may be found in the online version of this article.

**Correspondence to:**

E. Legrain,
etienne.legrain@ulb.be

**Citation:**

Legrain, E., Tollenaar, V., Goderis, S., Ardoin, L., Blard, P.-H., Claeys, P., et al. (2025). Absence of elevation-dependent warming in Antarctica inferred from blue ice paleoclimate records. *Geophysical Research Letters*, *52*, e2024GL113165. https://doi.org/10.1029/2024GL113165

Received 18 OCT 2024
Accepted 13 MAR 2025

**Author Contributions:**

**Conceptualization:** Etienne Legrain, Harry Zekollari
**Formal analysis:** Etienne Legrain, Veronica Tollenaar, Harry Zekollari
**Funding acquisition:** Veronica Tollenaar, Steven Goderis, Lisa Ardoin, Philippe Claeys, Vinciane Debaille, François Fripiat, Philippe Huybrechts, Naoya Imae, Frank Pattyn, Akira Yamaguchi, Harry Zekollari
**Investigation:** Etienne Legrain, Veronica Tollenaar, Steven Goderis, Lisa Ardoin, Pierre-Henri Blard, Philippe Claeys, Raúl R. Cordero, Vinciane Debaille, François Fripiat, Philippe Huybrechts, Maaike Izeboud, Frank Pattyn, Hamed Pourkhorsandi,



## 1. Introduction

Global warming has contrasting regional patterns, with amplified temperature changes at high latitude, a phenomenon known as "polar amplification" (Masson-Delmotte et al., 2006; Smith et al., 2019). Similarly, several studies have suggested that low-altitude warming may be amplified at high altitude (e.g., Garelick et al., 2022; Legrain et al., 2023; Mountain Research Initiative EDW Working Group, 2015). Since ice sheets and mountain glaciers are situated at high elevations, understanding how warming is amplified with altitude is crucial for

Julien Seguinot, Naoki Shirai, Marijke Vancappellen, Matthias Van Ginneken, Sarah Wauthy, Akira Yamaguchi, Mehmet Yesiltas, Harry Zekollari
**Methodology:** Etienne Legrain, Veronica Tollenaar, Steven Goderis, Harry Zekollari
**Resources:** Veronica Tollenaar, Steven Goderis, Philippe Claeys, Vinciane Debaille, François Fripiat, Philippe Huybrechts, Naoya Imae, Akira Yamaguchi, Harry Zekollari
**Writing – original draft:** Etienne Legrain, Veronica Tollenaar, Harry Zekollari
**Writing – review & editing:** Etienne Legrain, Veronica Tollenaar, Steven Goderis, Lisa Ardoin, Pierre-Henri Blard, Philippe Claeys, Raúl R. Cordero, Vinciane Debaille, François Fripiat, Philippe Huybrechts, Naoya Imae, Maaike Izeboud, Frank Pattyn, Hamed Pourkhorsandi, Julien Seguinot, Naoki Shirai, Marijke Vancappellen, Matthias Van Ginneken, Sarah Wauthy, Akira Yamaguchi, Mehmet Yesiltas, Harry Zekollari

predicting their response to climate change. Elevation-Dependent Warming (EDW) has been documented in several high-altitude mountainous regions over the past two decades (Mountain Research Initiative EDW Working Group, 2015; Wang et al., 2014; Williamson et al., 2020; Wu et al., 2023; You et al., 2020). Nevertheless, the scarcity of long-term high-altitude meteorological station observations drastically hampers the spatial and temporal characterization of EDW (Menne et al., 2018). To circumvent this issue, recent studies have used reanalysis data (Xie et al., 2023) and future projections from Global Climate Models (Zhu et al., 2024) to compute modern lapse rate (LR) over Antarctica. However, the two alternative approaches yielded opposing conclusions. The low signal-to-noise ratio of EDW also limits the detection of statistically relevant EDW patterns and the identification of key mechanisms (Mountain Research Initiative EDW Working Group, 2015).

Paleoclimatic studies can provide insights into the temporal and spatial sensitivity of EDW during past warming intervals. Several studies have investigated EDW during the last deglacial warming, which occurred between the Last Glacial Maximum (LGM, ~26–18 ka) and the Holocene (e.g., Hawaii: Blard et al., 2007; American cordillera: Legrain et al., 2023; East Africa: Loomis et al., 2017; Papua New Guinea: Tripati et al., 2014). During this deglaciation, sea-level temperature increased by 5–6°C (Clark et al., 2024; Tierney et al., 2020) with continental warming being approximately ~40% greater than over the ocean (Seltzer et al., 2023). By reconstructing specific site temperatures at different elevations, paleoclimatic studies allow determining a mean annual thermal LR along the surface slope. Whereas a change in the LR between the LGM and the Holocene (ΔLR) indicates either an attenuation or amplification of the high-altitude warming, a ΔLR close to zero implies a local absence of EDW. Paleoclimatic studies indicate the existence of regional-scale EDW spatial variability during the last deglacial warming (Blard et al., 2007; Legrain et al., 2023; Loomis et al., 2017; Tripati et al., 2014).

To date, all paleoclimatic studies on regional changes in LR and concurrent EDW have relied on paleotemperature reconstructions based on paleoglacier extents (e.g., Doughty et al., 2021), paleolake temperature (e.g., Garelick et al., 2022), and/or pollinic reconstruction (e.g., Van der Hammen & Hooghiemstra, 2000). Despite the diversity of used proxies, all these EDW reconstructions are restricted to the lower latitudes (40°N–40°S). Indeed, at higher latitudes, mountain glaciers and ice sheets reached very low altitudes during the LGM, in many cases covering the entire landscape (even at mid-latitudes, e.g., Seguinot et al., 2018). As a consequence, vegetation, lake, and/or frontal glacial moraines cannot be used at mid-to high latitudes to reconstruct high-elevation site paleotemperatures (Castillo-Llarena et al., 2023; Palacios et al., 2020). Outside the 40°N–40°S latitudinal range, past changes in local LR and the possible existence of EDW during major warming events are thus unknown.

Near the poles, the main paleotemperature proxies are the hydrogen and oxygen isotopic composition of ice (δD and $\delta^{18}O$ of $H_2O$), which correlate with the surface temperatures where the snow was deposited. Two approaches are used to reconstruct these temperature, using spatial (Jouzel et al., 2003; Masson-Delmotte et al., 2008) or temporal slope in ‰/°C (e.g., Buizert et al., 2021; Dahl-Jensen et al., 1999). Each ice core usually represents a single elevation, even if some sites could have evidenced significant elevation variations across glacial-interglacial periods, especially in West Antarctica (Buizert et al., 2021). As these elevation changes are also associated with change in temporality, deriving paleotemperatures across different elevations for a single time period is not feasible from a single ice core. While Greenland and Antarctic ice cores cover a wide range of elevations, their low spatial density poses a challenge for studying EDW. The interplay of multiple factors, such as latitude and regional climate, combined with elevation's influence on temperature changes, complicates isolating the specific effect of elevation on temperature.

In this study, we present a new approach to investigate deglacial EDW in Antarctica during a major climate warming event by analyzing the isotopic composition of surface blue ice samples. Blue ice areas (BIAs) make up for ~1% of the total Antarctic surface (Tollenaar et al., 2024) and are often explored for their potential to harbor large concentrations of meteorites (Cassidy et al., 1992; Tollenaar et al., 2022; Whillans & Cassidy, 1983). In these BIAs, old ice is directly exposed at the surface (in contrast to most of the continent that is covered by snow/firn) due to a combination of strong ablation processes driven by katabatic winds, and a specific bedrock topography that leads to a surface-directed vertical (i.e., upward) ice flow (Bintanja, 1999; Higgins et al., 2015; Sinisalo & Moore, 2010; Yan et al., 2019). As such, sampling surface ice in BIAs offers a unique method to reconstruct past climatic conditions across different time periods (Lee et al., 2022; Spaulding et al., 2013; Zekollari et al., 2019). Here, by sampling a variety of BIAs in and around an Antarctic mountainous range, we reconstruct LR changes during the last deglacial warming, thereby providing a first high-latitude EDW quantification between the LGM and the Holocene.

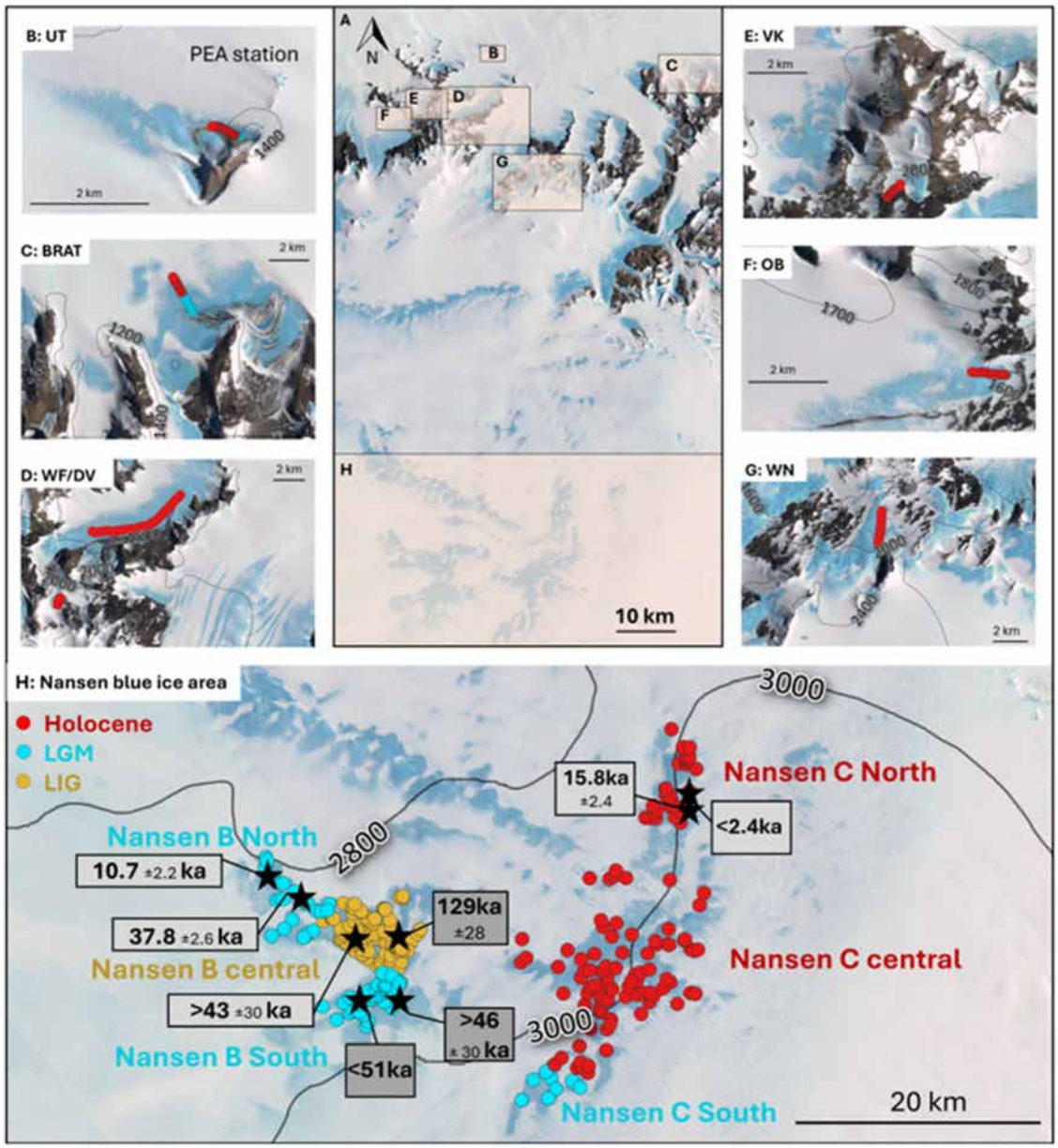


**Figure 1.** Surface blue ice samples collected in the Sør Rondane mountains (b–g) and Nansen blue ice field (h). (a) Overview of the study area. (b–h) Samples location along transects (b–g) and on the plateau (h) are represented by colored dots (legend in panel (h), with blue, red and orange dots representing the ice samples interpreted as belonging to Last Glacial Maximum (LGM), Holocene and Last Interglacial (LIG) periods, respectively). In panel (b), the blue star is the location of Princess Elisabeth Antarctica (PEA) station. In panel (h), the black stars represent dated meteorites from Zekollari et al. (2019). The corresponding light gray boxes denote the terrestrial ages as determined by $^{14}C$ dating, while the dark gray boxes correspond to the $^{36}Cl$ dated terrestrial ages. Background imagery are 15-m resolution Landsat images. The elevation contours are from the RAMP2 product (H. Liu et al., 2015). Data were plotted using the QGIS Quantarctica module (Matsuoka et al., 2021).

## 2. Field Sites and Campaigns

The studied sites are situated in and around the Sør Rondane Mountains, in Dronning Maud Land, East Antarctica, at latitudes between 71.8°S and 73.0°S and longitudes between 23.0°W and 24.5°W (Figure S1 in Supporting Information S1). These sites extend from around the Belgian Antarctic research station (Princess Elisabeth Antarctica, with the lower transect at an elevation of 1,100 m above sea level, m asl) and stretch up to ∼100 km southward, to the Nansen blue ice field (at elevations from ∼2,600 to ∼3,100 m asl, Figure 1). The Sør Rondane Mountains, which protrude from the ice sheet with elevations as high as 3,400 m asl, act as a transition between

the high-elevation East Antarctic plateau and the low-lying coastal area, leading to strong horizontal elevation gradients within a restricted area.

Here we rely on isotopic data measured from 617 blue ice samples, comprising 444 unpublished and 173 published $\delta^{18}O$ values (Zekollari et al., 2019), spanning a horizontal distance of 130 km and an elevation range from 1,050 to 3,063 m asl (Figure 1, Table S1 in Supporting Information S1). The data set comprises 276 samples collected from the Nansen blue ice field (plateau), and 341 samples collected along seven horizontal transects (over distances ranging from 500 to 6,000 m) in and around the Sør Rondane Mountains. Among the Nansen samples, 185 blue ice samples were collected during the BELARE 2012–13/JARE-54 expedition (Imae et al., 2015) and have already been published (Zekollari et al., 2019). All the other water isotopes data are new measurements of surface blue ice samples collected during four Antarctic field missions: (a) in 1989 (Brattnipane transect, "Brat," number of samples ($n$) = 81), (b) in 2012–2013 (Vikingshøgda transect, "VK," $n$ = 50; Otto Borchgrevinkfjellet transect, "OB," $n$ = 47; Utsteinen transect, "UT," $n$ = 90), (c) in 2018–2019, (DV, $n$ = 32; WF, $n$ = 22; WN, $n$ = 19), (d) in 2019–2020 ($n$ = 103, collected on the Nansen blue ice field) (Table S1 in Supporting Information S1).

## 3. Isotopic Signal

Blue ice samples were collected using a chisel, by removing the upper ~5 cm of surface ice, and then crushing the underlying ice below. The crushed ice was collected in small, sealed containers (50 ml) and transported in melted form for laboratory analysis. The $\delta^{18}O$ isotopic composition of the melted samples was analyzed at the Alfred Wegener Institute (AWI) for the samples collected close to Brattnipane (in 1989), while all other samples (collected in and after 2012) were analyzed at the Archeology, Environmental changes and GeoChemistry (AMGC) large research unit of the Vrije Universiteit Brussel (VUB) (see Supporting Information S1). When δD were also available, the mean isotopic values for each database location are well aligned on a local meteoric water line, with a slope of 7.82‰ ($R^2 = 0.99$) and 8.02‰ ($R^2 = 0.98$) for the Nansen blue ice field and the Sør Rondane mountains transects, respectively (Figure S2 in Supporting Information S1). This result indicates little to no fractionation and the preservation of the original signal. Among the seven transects, three (BRAT, UT, OB) exhibited a discernible spatial pattern in isotopic composition (Figures 2e–2g), with two distinct sections having an average amplitude change in the $\delta^{18}O$ composition larger than 5‰. This range of variation aligns with typical climatic glacial-interglacial range as observed from ice cores in Antarctica (Figure S3 in Supporting Information S1) (Buizert et al., 2021; Jouzel et al., 2007; Masson-Delmotte et al., 2011). In contrast, the isotopic composition of the four other transects (DV, WF, WN and VK) remains relatively stable throughout the transects, with values consistent with those expected during an interglacial period.

The central and northern parts of the Nansen C ice field exhibit $\delta^{18}O$ values with an average of $-40.6 \pm 1.4$‰ ($n$ = 98) and $-40.4 \pm 1.4$‰ ($n$ = 31), respectively, indicative of an interglacial climate (Figure 2h, Table S1 in Supporting Information S1). The southernmost sector of the Nansen C ice field is characterized by $\delta^{18}O$ values with an average value of $-45.1 \pm 0.9$‰ ($n$ = 5), indicative of a glacial climate (Figure 2h). Furthermore, both the northern and southern regions of the Nansen B ice field are composed of surface ice with isotopic values with average values of $-45.4 \pm 1.6$‰ ($n$ = 37) and $-45.6 \pm 1.6$‰ ($n$ = 22), respectively, indicative of a glacial climate (Figure 2h, Table S1 in Supporting Information S1).

## 4. Climate Periods Representative of the Blue Ice Transects

While some sections of the transects have been identified as belonging to interglacial or glacial periods based on their isotopic signatures, the exact climatic periods they correspond to are uncertain. To identify the corresponding time period, we performed four different types of analyses: (a) ice flow modeling, (b) statistical wiggle matching, (c) analyzing of high-resolution drone imagery, and (d) interpreting terrestrial ages of meteorites.

1. A 2D backtrack particle ice flow model was applied to the seven transects to estimate their likely age ranges (see Figures S4, S5, and Table S2 in Supporting Information S1). This model, widely used in BIA studies, provides an approximation of ice ages within the region (Grinsted et al., 2003; Kehrl et al., 2018). Although uncertainties in input parameters (surface velocity, mass balance, and ice thickness) do not allow for this approach to be used for absolute age dating for each transect, the estimated age magnitudes allow broadly linking specific transects to time periods. Notably, none of the simulated surface ages for the seven transects exceed 20,000 years (Figures S6, S7, and Table S2 in Supporting Information S1). Based on these results, it is

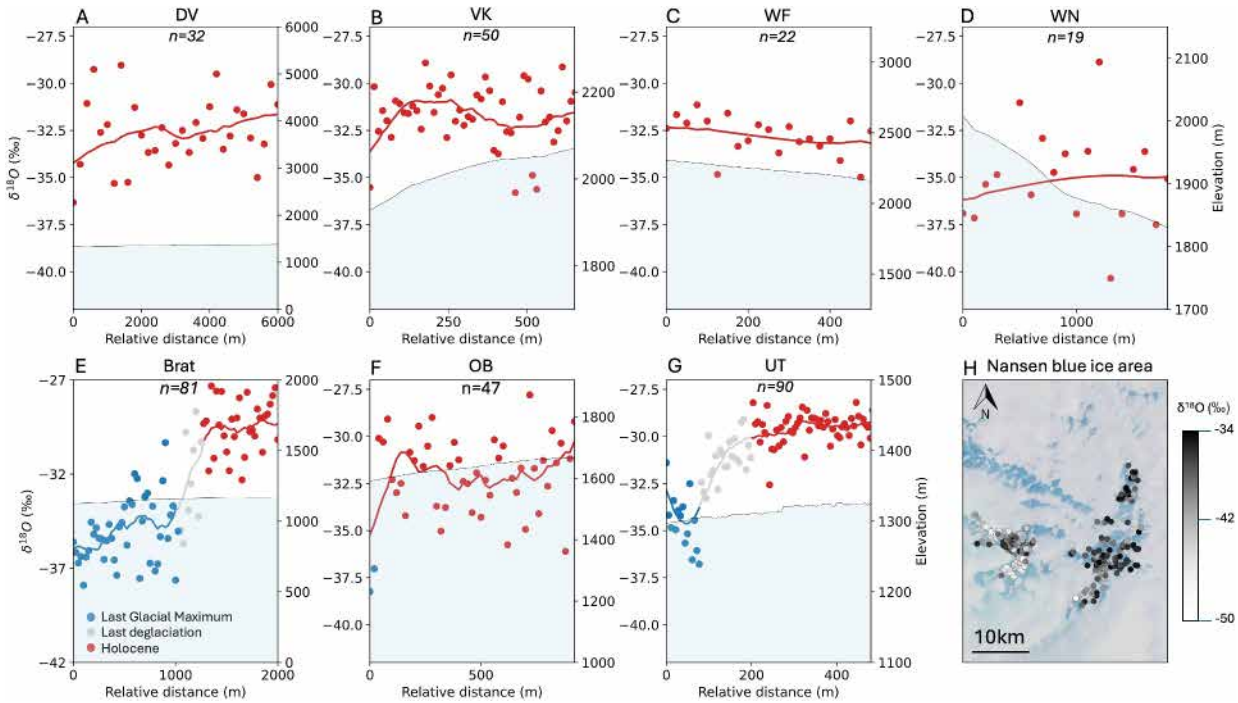


**Figure 2.** $\delta^{18}O$ values of ice samples along seven transects in the Sør Rondane mountains (a–g) and on the Nansen ice field (h). (a–g) Thick lines are smoothing splines computed with the Python module cspas (https://github.com/espdev/csaps) and used as a high-pass filter to only preserve the orbital-scale climate variability in the ice isotopes record. Blue, gray and red colors refer to $\delta^{18}O$ values associated to glacial, deglacial and interglacial periods respectively. Light blue shaded areas are the sampling elevation profiles along the transect.

highly likely that the interglacial signatures of the transects correspond to the Holocene. Furthermore, the lack of isotopic variability within the interglacial composition is a defining feature of the Holocene, a stable climatic period, in contrast to the more abrupt isotopic patterns observed in the Last Interglacial (Figure S6 in Supporting Information S1). Consequently, all seven interglacial $\delta^{18}O$ sections are interpreted as representing the current interglacial period (Holocene, 11.7–0 ka), whereas the two transects that transition into a glacial period contain ice from the end of this period, roughly corresponding to the LGM (Supporting Information S1).

2. Similarity analyses linking a reference curve (EDML $\delta^{18}O$ record: Stenni et al., 2010) to the signal obtained from the transects were performed using wiggle-matching for the three transects that show a potential glacial/interglacial transitions (OB transect, UT transect, and Brat transect). A heatmap illustrating the $R^2$ correlation between the reference (EDML) and tested records is shown in Figure S6 in Supporting Information S1. For the UT and Brat transects, this wiggle-matching analysis strongly supports the hypothesized transition including ice from the LGM, the last deglaciation, and the Holocene. However, the results for the OB transect were inconclusive. Consequently, we do not consider this transect representative of a deglaciation phase and instead only rely on the Holocene section of the transect for further analyses.
3. During the BELSPO FROID Antarctic mission 2024/2025, high-resolution drone imagery was acquired along the UT transect to investigate the occurrence of potential discontinuities in the surface ice record. Visible ash and ice layers show no evidence of folding or faulting, suggesting that the blue ice in this area is continuous at the surface (Figure S7 in Supporting Information S1).
4. Interpreting the isotopic signals from the Nansen blue ice field is challenging, as the samples were not collected along transects but are instead randomly distributed (Figures 1 and 2h). However, terrestrial ages from meteorites collected on the ice field are available (Zekollari et al., 2019). While ages of meteorites are not equivalent to surface ice age, they are good indicators to attribute clusters of isotopic values to specific climate periods (Sinisalo & Moore, 2010; Zekollari et al., 2019). The terrestrial meteorite ages in this area date back to the Holocene and the LGM period (Zekollari et al., 2019) (Figure 1). Finally, the central part of the Nansen B ice field exhibits isotopic values with an average of $-41.9 \pm 1.7‰$ ($n = 83$), indicative of an interglacial period. Nevertheless, the meteorite ages in this region (129 ± 28 ka) suggest that the ice within this specific

area of the Nansen blue ice field is most likely from the Last Interglacial rather than the Holocene. Consequently, the central part of the Nansen B icefield is not included in the following analyses.

## 5. Temperature Signal Derived From Isotopic Composition

Surface temperature estimates are derived from $\delta^{18}O$ values using the relationship from Masson-Delmotte et al. (2008) of $\delta^{18}O = 0.80 \times T - 8.11$, where T denotes the mean annual surface temperature in °C. This calibration was established from a data set covering the whole Antarctic continent. Although regional variations in the linear relationship between $\delta^{18}O$ values and site temperature have been observed (Masson-Delmotte et al., 2008; Touzeau et al., 2016), the conversion factor determined locally for the Dome Fuji site (77.50°S, 39.70°E), which is approximately 700 km from the studied site, closely matches the global Antarctic value ($0.76 \pm 0.02‰\ C^{-1}$ against $0.80 \pm 0.01‰\ C^{-1}$; Dittmann et al., 2016). This comparison gives us confidence in using the global Antarctic conversion factor at our location. The selected value for the conversion factor does not affect the comparison of the vertical gradient of temperature between the glacial and the interglacial periods, as the same coefficient is applied uniformly across all our investigated sites. The computed site temperature, which is representative for the mean annual surface temperature at the site of snow deposition, is on average (over all samples) $-33.1 \pm 5.7$°C ($1\sigma$) for the Holocene, and $-40.6 \pm 6.6$°C ($1\sigma$) for the LGM (Table S1 in Supporting Information S1). Continuous temperature measurements from two weathers stations, PE_AIR and PE_GUN, are available in the area at similar elevation range (1,382 and 2,346 m asl). The mean annual temperatures (−18.7 and −27.9°C) are slightly warmer by 4.6°C on average, ranging from 1.6 to 8.1°C, compared to interglacial temperatures derived from blue ice sites located at similar elevation (Table S1 in Supporting Information S1). This discrepancy could be explained by the global Antarctic difference of temperature between the period of measurement (2015–2019) and the interglacial period. In addition, it could reveal a potential overestimation of the calibration coefficient of $0.8‰\ C^{-1}$ used in this study to convert isotopic signal into temperature. Nevertheless, the order of magnitude of temperature range is similar between the measured temperature and the isotopes-derived temperature.

## 6. Source Elevation Identification

To link the derived temperatures to surface elevations, we identify the original location where the ice once fell as snow precipitation before compaction and displacement by flowing (Jouzel et al., 1997). To this end, we use the MEaSUREs surface ice velocities (Mouginot et al., 2012) and the RAMP2 surface elevation model (H. Liu et al., 2015) both available in the QGIS Quantarctica module (Matsuoka et al., 2021). Using this approach, we determine the most likely deposition elevation for each of the identified glacial-interglacial clusters, computing it as a broad range to account for the associated uncertainties (Figure S8 and Table S1 in Supporting Information S1). The elevation range was estimated using the maximum surface elevation in the potential accumulation area and considering the gradient of surface elevation (details provided in Supporting Information S1). In the specific case of the Nansen area, ice flow modeling provides an additional constraint for the original area of deposit (Zekollari et al., 2019).

To account for possible changes in ice sheet elevation over time, we rely on cosmic-ray exposure ages in the Sør Rondane mountains, which suggests that the ice sheet surface was 50 m higher during the LGM (Suganuma et al., 2014). Therefore, to compute the elevation of the LGM samples, a correction was applied by adding 50 m to the altitude for the Holocene samples. For the Sør Rondane surface transects, the seven deposition-site elevations range from $1{,}100 \pm 50$ m asl to $2{,}600 \pm 100$ m asl during the Holocene. For the LGM samples, the three deposition-site elevations range from $1{,}150 \pm 50$ m asl to $1{,}700 \pm 50$ m asl (Figure S8 and Table S1 in Supporting Information S1). For the Nansen ice field, a previous study estimated the source elevation for the Holocene ice to be $3{,}100 \pm 100$ m asl based on 2D ice flow modeling (Zekollari et al., 2019). For Nansen, by applying the 50 m correction, we thus estimate the LGM source site elevation to be at $3{,}150 \pm 100$ m asl (Table S1 in Supporting Information S1).

## 7. Lapse Rate Computation and Elevation-Dependent Warming

In most studies, paleo LR estimates are computed through paleoelevation and paleotemperature calculated from contrasting high-altitude (e.g., paleo-equilibrium line altitude of a glacier) and low-altitude (e.g., sea surface temperature) sites (e.g., Blard et al., 2007; Legrain et al., 2023; Tripati et al., 2014). In this study, we present a new

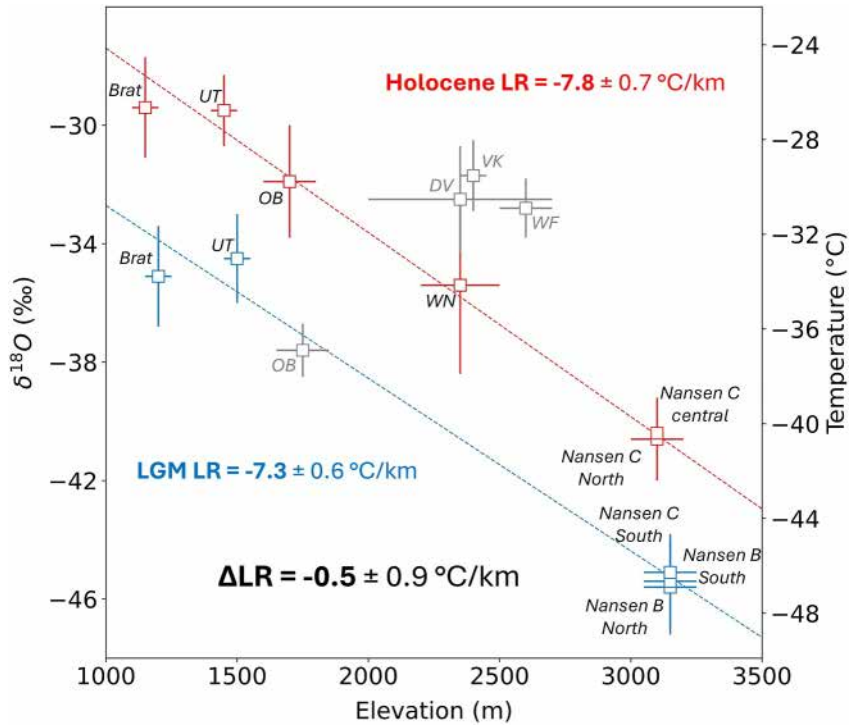


**Figure 3.** Dependence of temperature on elevation. Each square corresponds to a (sub)transect or a region as defined in Figure 1. Blue squares represent palaeoelevations and paleotemperature reconstructions from the Last Glacial Maximum (LGM), while red squares represent the Holocene period. The range of possible source elevations and the range of $\delta^{18}O$ (/temperatures) for a given (sub)transect are represented by horizontal and vertical bars, respectively. The four light gray squares are Holocene/LGM data that were not included for the Holocene/LGM linear regression due to local climatic conditions (Holocene, VK, DV, WF, detailed in Section 5) and uncertainty of dating (LGM, OB). Dashed blue/red lines are linear regressions for the Holocene/LGM data sets. The conversion factor between $\delta^{18}O$ values and temperature of $0.8‰.C^{-1}$ is from Masson-Delmotte et al. (2008). LGM, Last Glacial Maximum; LR, mean annual thermal lapse rate along the slope.

method that relies on more than two sites, offering a statistically robust estimate of the paleo LR variations. More specifically, we perform regression analyses using temperature and elevation data from nine Holocene sites and six LGM sites, respectively (Figure 3). Here, we find a notably lower coefficient of correlation for the Holocene ($R^2 = 0.76$) compared to the LGM ($R^2 = 0.98$) (Figure 3).

For the Holocene, the three sites located in high-mountainous relief (VK, WN, DV) deviate from the general elevation versus temperature pattern of the region. The higher reconstructed temperatures are interpreted as being indicative of a microclimate within the valley, where local wind patterns may be altered by the mountainous topography and albedo values are lower due to exposed bedrock (Takahashi et al., 1992) (Figure 2, Figure S8 in Supporting Information S1). Unlike the other transects situated in more open environments, we hypothesize that the surrounding relief likely shielded this area from the katabatic winds that are typical for the region, thereby possibly facilitating the formation and persistence of a cloud cover in the vicinity. An alternative hypothesis in which the ice was not deposited during the Holocene but rather during the Last Interglacial, which is warmer than the Holocene period (Past Interglacials Working Group of PAGES, 2016), is not deemed realistic. The steep slopes in this area result in a high surface velocity and do not allow for old ice to stagnate at these locations. Therefore, we consider these three anomalous sites (VK, WN and DV) as outliers and exclude them from the elevation *vs*. temperature regression, after which the temperature-elevation relationship becomes much stronger ($R^2 = 0.97$ with the six remaining sites).

The reconstructed LR values for the Holocene and LGM periods, $-7.8 \pm 0.7°C\ km^{-1}$ and $-7.2 \pm 0.5°C\ km^{-1}$ respectively (Figure 3), are realistic in comparison to modern LR value derived from three weather stations located in the studied area ($-7.9 \pm 0.9°C.km^{-1}$; Table S3 in Supporting Information S1). In our study area, the change in LR between LGM and Holocene (ΔLR) is almost nonexistent ($-0.6 \pm 0.9°C\ km^{-1}$; not significantly ($1\sigma$) different from zero), implying that there is very little to no EDW in this area. Note that if we repeat the analyses with the three excluded high-mountain sites, ΔLR is $0.5 \pm 1.8°C\ km^{-1}$, which still implies an absence of

EDW in the area. An analysis demonstrating the absence of sensitivity of our main results to computational choices (exclusion of sites, isotopic calibration factor, source elevation correction) is presented in Supplementary Materials (Text S5 in Supporting Information S1) and in Figure S9 in Supporting Information S1.

## 8. Discussion

The absence of EDW in this region of Antarctica during the last deglacial warming contrasts with most of the lower-latitudes regions that were subject to a clear amplification of warming at high elevation during this time interval (e.g., Hawaii: Blard et al., 2007; East Africa: Garelick et al., 2022; Tropical Andes: Legrain et al., 2023). Over the instrumental period, most of the mountainous areas in the world are experiencing an amplification of warming with increasing elevation (Mountain Research Initiative EDW Working Group, 2015; Wang et al., 2014). However, the scarcity of high-elevation climate stations in Antarctica hampers establishing a direct relationship between elevation and mean annual temperature changes. To address this challenge, two recent studies have employed alternative approaches to circumvent some of the limitations of direct observations, using (a) reanalysis data from the 1958–2020 period (ERA5 product, Xie et al., 2023) and (b) future projections from Global Climate Models (GCMs) over the 2015–2100 period (CMIP6, Zhu et al., 2024). The two alternative approaches yielded opposing conclusions. While the reanalysis approach suggested an attenuation of the recent warming with elevation, that is, a negative EDW, the GCMs approach showed a future amplification of the warming with elevation, that is, a positive EDW. A crucial methodological aspect and possible limitation in these approaches is that they compute averages across the entire continent, necessitating a deconvolution of the elevation and latitude effects on temperature, resulting in large uncertainties. In contrast, our approach overcomes this issue by comparing high and low elevation sites located at very close proximity. This key methodological difference may explain discrepancies between our study and the two other contrasting studies, although a part of the differences may also be linked to different time periods studied, where we focus on glacial-interglacial timescales as opposed to recent past and future periods.

To understand the absence of EDW in this region of Antarctica during a major warming event as revealed in our study, we analyze the potential drivers for a LR change. Although these drivers (e.g., albedo, aerosols, moisture content, meridional heat transport) are still debated (Mountain Research Initiative EDW Working Group, 2015), we can propose two primary mechanisms.

1. *Moisture content*. Based on paleoproxy reconstructions, Legrain et al. (2023) found a strong positive relationship between the occurrence of positive EDW and the increase of mean annual precipitation during the last deglacial warming derived from paleoproxies. Through a modeling approach, they confirmed the role of specific moisture, closely correlated with mean annual precipitation, as a driver for LR variations over the last deglacial warming. These changes in moisture content have also been identified as a key mechanism to explain EDW patterns under ongoing global warming (Mountain Research Initiative EDW Working Group, 2015). Linking moisture and precipitation changes with LR changes in our study area is not possible since proxy-based reconstruction of LGM paleo-precipitation are lacking. An alternative approach consists of relying on LGM global climate modeling efforts, such as those included in the Paleoclimate Modeling Intercomparison Project (PMIP4; Kageyama et al., 2021). In PMIP4, most of climate models yield significantly wetter Pre-Industrial (PI) Holocene conditions compared to the LGM, with, on average, a 88 ± 79 % ($1\sigma$) increase in mean annual precipitation in our studied area (Figure S10 in Supporting Information S1). Despite this pronounced relative increase of precipitation, the total amount of precipitation remains low, increasing from 128 ± 51 mm $yr^{-1}$ during the LGM to ∼234 ± 116 mm $yr^{-1}$ during the PI time period. Using the relationship between the changes in mean annual precipitation and LR ($\Delta LR = 0.0024 \cdot \Delta P + 0.17$ from Legrain et al., 2023), an increase in LR between LGM and PI of 0.4 ± 0.4°C $km^{-1}$ is predicted. This very limited (positive) change in LR agrees, within uncertainties, with our reconstructed LR change of −0.6 ± 0.9°C $km^{-1}$. However, this interpretation should be considered with caution because (a) there are large uncertainties in paleoprecipitation model estimates, and (b) the original relationship was calibrated to data from low-latitude areas.
2. *Surface albedo*. Previous studies have highlighted how surface albedo changes affect the amount of solar irradiance absorbed by the ground surface and thereby have the potential to substantially affect the LR (Minder et al., 2018; Palazzi et al., 2019; Zhu et al., 2024). Currently, an estimated 99.6 % of the Antarctic continent is covered by snow or ice (Brooks et al., 2019). Given the strongly negative mean annual temperatures in East Antarctica, significant variations in snow coverage at the continent-scale during deglacial warming are

unlikely (Seo et al., 2016; Van Den Broeke et al., 1999). Although increased dust deposition during cold periods in Antarctica may impact albedo, its effect is believed to be of secondary importance (Y. Liu et al., 2013). The lack of potential for snow cover changes to occur during a warming event in Antarctica, contrasting with most of other high-elevation regions on Earth, may partly explain the absence of EDW Antarctica. However, in our study area, a substantial part of the surface consists of rocks (mostly granitoids and metamorphic rocks) or blue ice, both with lower albedos compared to snow. In the Sør Rondane Mountains, the warming of the last deglaciation and the associated increase in snowfall thus has the potential to reduce the extent of blue ice and rock-covered surface at high elevation, increasing the temperature while remaining below zero and resulting in higher albedo. At lower elevation, an increase of temperature results occasionally in temperature to exceed zero during summer warm episodes, causing melting event that diminished snow cover and counterbalance exceed in precipitation. Although the magnitude of the albedo changes is limited overall, locally it could contribute to a small decrease in EDW. Consequently, it may have balanced the slight EDW triggered by increased moisture in the atmosphere.

In summary, we propose that the absence of EDW in the study area probably results from a combination of the effects of moisture and albedo changes, which have opposite impacts in this area (Figure S11 in Supporting Information S1). Nevertheless, Buizert et al. (2021) suggest that during the LGM, the strong surface-based temperature inversions observed in modern Antarctica may have been altered, potentially influencing the temporal variability of the LR. These inversions, driven by radiative cooling, are particularly pronounced in the cold, stable boundary layer of East Antarctica. Changes in inversion strength during glacial periods could contribute to differences between temporal and spatial temperature gradients (Buizert et al., 2021). Additional mechanisms, specific to Antarctica, could further complicate the identification of causes for the LR reconstruction in our study. Further research on the stability of these inversion layers over glacial periods is required to better constrain their impact on LR variations in Antarctic regions during this time.

The absence of post-LGM EDW in this region of Antarctica during the last deglacial warming underscores the importance of considering local climatic factors when assessing how warming might amplify or reduce with elevation. While EDW has been documented in various mountainous regions in tropical to mid-latitude regions across the globe (e.g., Legrain et al., 2023; Liu et al., 2023), the potential absence of this phenomenon in Antarctica suggests that different mechanisms may govern the elevation-temperature relationship in high-latitude polar environments, where the increase of temperature does not impact the snowline elevation. Nevertheless, it can not be excluded that some of our findings do not apply to other parts of the continent that are not constrained by local topographic effects specific to blue ice and mountainous areas of Antarctica. As we here provide the first LR reconstruction over the LGM in Antarctica, further sites must be investigated to constrain the potential intra-continental variability of LR changes. A recent study estimated the global average atmospheric LGM LR using the proportional abundance of $^{18}O^{18}O$ in $O_2$ in polar ice cores to constrain the average temperature of the upper troposphere, suggesting a nearly negligible LR change since the LGM (Banerjee et al., 2022). The contrasting EDW pattern between the Tropics (e.g., Blard et al., 2007; Legrain et al., 2023; Loomis et al., 2017), the high-latitudes (this study) and the global climate regions (Banerjee et al., 2022) may underline a compensatory mechanism that buffered the post-LGM EDW observed in several tropical regions.

## Data Availability Statement

Ice isotopes data used in this study are available to download at Legrain (2025).

**Acknowledgments**
This study is an outcome of the Finding the world's oldest ice record around the Princess Elisabeth Station (FROID) project. It received the financial and logistical support from the Belgian Science Policy Office (BELSPO) and International Polar Fundation (IPF). E.L. was funded by the FROID project. V.T. was funded by an FNRS PhD fellowship and a junior postdoctoral fellowship of the Research Foundation—Flanders (FWO). H.Z. and M.I. were supported through funding received from the European Research Council (ERC) under the European Union's Horizon Framework research and innovation programme (Grant agreement 101115565; "ICE$^3$" project). H.Z. was also supported through a VUB ZAP Startkrediet ("ICEFIELD" project). P.C, V.D. and S.G. received funding from BELSPO Brain.be projects BAMM, Diabas, Amundsen, DESIRED and ULTIM. J.S. and H.Z. acknowledge the funding received from the research foundation—Flanders (FWO) through an Odysseus Type II project (Grant agreement G0DCA23N; "GlaciersMD" project). V.D. is supported by FRS-FNRS. R.R.C. acknowledges FONDECYT 1231904 and ANILLO ACT210046. P.C. & S.G. acknowledge support from VUB Strategic Research and Research Foundation Flanders (FWO-HERC46) for maintenance and purchase of instruments.

## References

Banerjee, A., Yeung, L. Y., Murray, L. T., Tie, X., Tierney, J. E., & Legrande, A. N. (2022). Clumped-isotope constraint on upper-tropospheric cooling during the last glacial maximum. *AGU Advances*, *3*(4), e2022AV000688. https://doi.org/10.1029/2022AV000688

Bintanja, R. (1999). On the glaciological, meteorological, and climatological significance of Antarctic blue ice areas. *Reviews of Geophysics*, *37*(3), 337–359. https://doi.org/10.1029/1999RG900007

Blard, P.-H., Lavé, J., Pik, R., Wagnon, P., & Bourlès, D. (2007). Persistence of full glacial conditions in the central Pacific until 15,000 years ago. *Nature*, *449*(7162), 591–594. https://doi.org/10.1038/nature06142

Brooks, S. T., Jabour, J., Van Den Hoff, J., & Bergstrom, D. M. (2019). Our footprint on Antarctica competes with nature for rare ice-free land. *Nature Sustainability*, *2*(3), 185–190. https://doi.org/10.1038/s41893-019-0237-y

Buizert, C., Fudge, T. J., Roberts, W. H. G., Steig, E. J., Sherriff-Tadano, S., Ritz, C., et al. (2021). Antarctic surface temperature and elevation during the last glacial maximum. *Science*, *372*(6546), 1097–1101. https://doi.org/10.1126/science.abd2897

Cassidy, W., Harvey, R., Schutt, J., Delisle, G., & Yanai, K. (1992). The meteorite collection sites of Antarctica. *Meteoritics*, *27*(5), 490–525. https://doi.org/10.1111/j.1945-5100.1992.tb01073.x

Castillo-Llarena, A., Retamal-Ramírez, F., Bernales, J., Jacques-Coper, M., & Rogozhina, I. (2023). Climate and ice sheet dynamics in Patagonia during the last glacial maximum. *Climate of the Past Discussions*, *2023*, 1–26. https://doi.org/10.5194/cp-2023-47

Clark, P. U., Shakun, J. D., Rosenthal, Y., Köhler, P., & Bartlein, P. J. (2024). Global and regional temperature change over the past 4.5 million years. *Science*, *383*(6685), 884–890. https://doi.org/10.1126/science.adi1908

Dahl-Jensen, D., Morgan, V. I., & Elcheikh, A. (1999). Monte Carlo inverse modelling of the Law Dome (Antarctica) temperature profile. *Annals of Glaciology*, *29*, 145–150. https://doi.org/10.3189/172756499781821102

Dittmann, A., Schlosser, E., Masson-Delmotte, V., Powers, J. G., Manning, K. W., Werner, M., & Fujita, K. (2016). Precipitation regime and stable isotopes at Dome Fuji, East Antarctica. *Atmospheric Chemistry and Physics*, *16*(11), 6883–6900. https://doi.org/10.5194/acp-16-6883-2016

Doughty, A. M., Kaplan, M. R., Peltier, C., & Barker, S. (2021). A maximum in global glacier extent during MIS 4. *Quaternary Science Reviews*, *261*, 106948. https://doi.org/10.1016/j.quascirev.2021.106948

Garelick, S., Russell, J., Richards, A., Smith, J., Kelly, M., Anderson, N., et al. (2022). The dynamics of warming during the last deglaciation in high-elevation regions of Eastern Equatorial Africa. *Quaternary Science Reviews*, *281*, 107416. https://doi.org/10.1016/j.quascirev.2022.107416

Grinsted, A., Moore, J., Spikes, V. B., & Sinisalo, A. (2003). Dating Antarctic blue ice areas using a novel ice flow model. *Geophysical Research Letters*, *30*(19), 2003GL017957. https://doi.org/10.1029/2003GL017957

Higgins, J. A., Kurbatov, A. V., Spaulding, N. E., Brook, E., Introne, D. S., Chimiak, L. M., et al. (2015). Atmospheric composition 1 million years ago from blue ice in the Allan Hills, Antarctica. *Proceedings of the National Academy of Sciences*, *112*(22), 6887–6891. https://doi.org/10.1073/pnas.1420232112

Imae, N., Debaille, V., Akada, Y., Debouge, W., Goderis, S., Hublet, G., et al. (2015). Report of the JARE-54 and BELARE 2012–2013 joint expedition to collect meteorites on the Nansen Ice Field, Antarctica. *Antarctic Record*, *59*(1), 38–72.

Jouzel, J., Alley, R. B., Cuffey, K. M., Dansgaard, W., Grootes, P., Hoffmann, G., et al. (1997). Validity of the temperature reconstruction from water isotopes in ice cores. *Journal of Geophysical Research*, *102*(C12), 26471–26487. https://doi.org/10.1029/97JC01283

Jouzel, J., Masson-Delmotte, V., Cattani, O., Dreyfus, G., Falourd, S., Hoffmann, G., et al. (2007). Orbital and millennial Antarctic climate variability over the past 800,000 years. *Science*, *317*(5839), 793–796. https://doi.org/10.1126/science.1141038

Jouzel, J., Vimeux, F., Caillon, N., Delaygue, G., Hoffmann, G., Masson-Delmotte, V., & Parrenin, F. (2003). Magnitude of isotope/temperature scaling for interpretation of central Antarctic ice cores. *Journal of Geophysical Research*, *108*(D12), 2002JD002677. https://doi.org/10.1029/2002JD002677

Kageyama, M., Harrison, S. P., Kapsch, M.-L., Lofverstrom, M., Lora, J. M., Mikolajewicz, U., et al. (2021). The PMIP4 last glacial maximum experiments: Preliminary results and comparison with the PMIP3 simulations. *Climate of the Past*, *17*(3), 1065–1089. https://doi.org/10.5194/cp-17-1065-2021

Kehrl, L., Conway, H., Holschuh, N., Campbell, S., Kurbatov, A. V., & Spaulding, N. E. (2018). Evaluating the duration and continuity of potential climate records from the Allan Hills Blue Ice Area, East Antarctica. *Geophysical Research Letters*, *45*(9), 4096–4104. https://doi.org/10.1029/2018GL077511

Lee, G., Ahn, J., Ju, H., Ritterbusch, F., Oyabu, I., Buizert, C., et al. (2022). Chronostratigraphy of the Larsen blue-ice area in northern Victoria Land, East Antarctica, and its implications for paleoclimate. *The Cryosphere*, *16*(6), 2301–2324. https://doi.org/10.5194/tc-16-2301-2022

Legrain, E. (2025). EtienneLegrainULB/Legrain2025_GRL_IceIsotopes: Legrain2025_GRL_IceIsotopes (vf). [Dataset]. *Zenodo*. https://doi.org/10.5281/zenodo.15273585

Legrain, E., Blard, P.-H., Kageyama, M., Charreau, J., Leduc, G., Bourdin, S., & Bekaert, D. V. (2023). Moisture amplification of the high-altitude deglacial warming. *Quaternary Science Reviews*, *318*, 108303. https://doi.org/10.1016/j.quascirev.2023.108303

Liu, H., Jezek, K., Li, B., & Zhao, Z. (2015). Radarsat Antarctic mapping project digital elevation model, version 2. *NASA National Snow and Ice Data Center Distributed Active Archive Center*. https://doi.org/10.5067/8JKNEW6BFRVD

Liu, Y., Shi, G., & Xie, Y. (2013). Impact of dust aerosol on glacial-interglacial climate. *Advances in Atmospheric Sciences*, *30*(6), 1725–1731. https://doi.org/10.1007/s00376-013-2289-7

Liu, Z., Bao, Y., Thompson, L. G., Mosley-Thompson, E., Tabor, C., Zhang, G. J., et al. (2023). Tropical mountain ice core $\delta^{18}$O: A Goldilocks indicator for global temperature change. *Science Advances*, *9*(45), eadi6725. https://doi.org/10.1126/sciadv.adi6725

Loomis, S. E., Russell, J. M., Verschuren, D., Morrill, C., De Cort, G., Sinninghe Damsté, J. S., et al. (2017). The tropical lapse rate steepened during the Last Glacial Maximum. *Science Advances*, *3*(1), e1600815. https://doi.org/10.1126/sciadv.1600815

Masson-Delmotte, V., Buiron, D., Ekaykin, A., Frezzotti, M., Gallée, H., Jouzel, J., et al. (2011). A comparison of the present and last interglacial periods in six Antarctic ice cores. *Climate of the Past*, *7*(2), 397–423. https://doi.org/10.5194/cp-7-397-2011

Masson-Delmotte, V., Hou, S., Ekaykin, A., Jouzel, J., Aristarain, A., Bernardo, R. T., et al. (2008). A review of Antarctic surface snow isotopic composition: Observations, atmospheric circulation, and isotopic modeling. *Journal of Climate*, *21*(13), 3359–3387. https://doi.org/10.1175/2007JCLI2139.1

Masson-Delmotte, V., Kageyama, M., Braconnot, P., Charbit, S., Krinner, G., Ritz, C., et al. (2006). Past and future polar amplification of climate change: Climate model intercomparisons and ice-core constraints. *Climate Dynamics*, *26*(5), 513–529. https://doi.org/10.1007/s00382-005-0081-9

Matsuoka, K., Skoglund, A., Roth, G., De Pomereu, J., Griffiths, H., Headland, R., et al. (2021). Quantarctica, an integrated mapping environment for Antarctica, the Southern Ocean, and sub-Antarctic islands. *Environmental Modelling & Software*, *140*, 105015. https://doi.org/10.1016/j.envsoft.2021.105015

Menne, M. J., Williams, C. N., Gleason, B. E., Rennie, J. J., & Lawrimore, J. H. (2018). The global historical climatology network monthly temperature dataset, version 4. *Journal of Climate*, *31*(24), 9835–9854. https://doi.org/10.1175/JCLI-D-18-0094.1

Minder, J. R., Letcher, T. W., & Liu, C. (2018). The character and causes of elevation-dependent warming in high-resolution simulations of rocky mountain climate change. *Journal of Climate*, *31*(6), 2093–2113. https://doi.org/10.1175/JCLI-D-17-0321.1

Mouginot, J., Scheuchl, B., & Rignot, E. (2012). Mapping of ice motion in Antarctica using synthetic-aperture radar data. *Remote Sensing*, *4*(9), 2753–2767. https://doi.org/10.3390/rs4092753

Mountain Research Initiative EDW Working Group. (2015). Elevation-dependent warming in mountain regions of the world. *Nature Climate Change*, *5*(5), 424–430. https://doi.org/10.1038/nclimate2563

Palacios, D., Stokes, C. R., Phillips, F. M., Clague, J. J., Alcalá-Reygosa, J., Andrés, N., et al. (2020). The deglaciation of the Americas during the last glacial termination. *Earth-Science Reviews*, *203*, 103113. https://doi.org/10.1016/j.earscirev.2020.103113

Palazzi, E., Mortarini, L., Terzago, S., & Von Hardenberg, J. (2019). Elevation-dependent warming in global climate model simulations at high spatial resolution. *Climate Dynamics*, *52*(5–6), 2685–2702. https://doi.org/10.1007/s00382-018-4287-z

Past Interglacials Working Group of PAGES. (2016). Interglacials of the last 800,000 years. *Reviews of Geophysics*, *54*(1), 162–219. https://doi.org/10.1002/2015RG000482

Seguinot, J., Ivy-Ochs, S., Jouvet, G., Huss, M., Funk, M., & Preusser, F. (2018). Modelling last glacial cycle ice dynamics in the Alps. *The Cryosphere*, *12*(10), 3265–3285. https://doi.org/10.5194/tc-12-3265-2018

Seltzer, A. M., Blard, P.-H., Sherwood, S. C., & Kageyama, M. (2023). Terrestrial amplification of past, present, and future climate change. *Science Advances*, *9*(6), eadf8119. https://doi.org/10.1126/sciadv.adf8119

Seo, M., Kim, H.-C., Huh, M., Yeom, J.-M., Lee, C., Lee, K.-S., et al. (2016). Long-term variability of surface albedo and its correlation with climatic variables over Antarctica. *Remote Sensing*, *8*(12), 981. https://doi.org/10.3390/rs8120981

Sinisalo, A., & Moore, J. C. (2010). Antarctic blue ice areas - Towards extracting palaeoclimate information. *Antarctic Science*, *22*(2), 99–115. https://doi.org/10.1017/S0954102009990691

Smith, D. M., Screen, J. A., Deser, C., Cohen, J., Fyfe, J. C., García-Serrano, J., et al. (2019). The polar amplification model Intercomparison project (PAMIP) contribution to CMIP6: Investigating the causes and consequences of polar amplification. *Geoscientific Model Development*, *12*(3), 1139–1164. https://doi.org/10.5194/gmd-12-1139-2019

Spaulding, N. E., Higgins, J. A., Kurbatov, A. V., Bender, M. L., Arcone, S. A., Campbell, S., et al. (2013). Climate archives from 90 to 250 ka in horizontal and vertical ice cores from the Allan Hills Blue Ice Area, Antarctica. *Quaternary Research*, *80*(3), 562–574. https://doi.org/10.1016/j.yqres.2013.07.004

Stenni, B., Masson-Delmotte, V., Selmo, E., Oerter, H., Meyer, H., Röthlisberger, R., et al. (2010). The deuterium excess records of EPICA Dome C and Dronning Maud Land ice cores (East Antarctica). *Quaternary Science Reviews*, *29*(1–2), 146–159. https://doi.org/10.1016/j.quascirev.2009.10.009

Suganuma, Y., Miura, H., Zondervan, A., & Okuno, J. (2014). East Antarctic deglaciation and the link to global cooling during the Quaternary: Evidence from glacial geomorphology and 10Be surface exposure dating of the Sør Rondane Mountains, Dronning Maud Land. *Quaternary Science Reviews*, *97*, 102–120. https://doi.org/10.1016/j.quascirev.2014.05.007

Takahashi, S., Endoh, T., Azuma, N., & Meshida, S. (1992). Bare ice fields developed in the inland. *Proceedings of the NIPR Symposium on Polar Meteorology and Glaciology*, *5*, 128–139.

Tierney, J. E., Zhu, J., King, J., Malevich, S. B., Hakim, G. J., & Poulsen, C. J. (2020). Glacial cooling and climate sensitivity revisited. *Nature*, *584*(7822), 569–573. https://doi.org/10.1038/s41586-020-2617-x

Tollenaar, V., Zekollari, H., Lhermitte, S., Tax, D. M. J., Debaille, V., Goderis, S., et al. (2022). Unexplored Antarctic meteorite collection sites revealed through machine learning. *Science Advances*, *8*(4), eabj8138. https://doi.org/10.1126/sciadv.abj8138

Tollenaar, V., Zekollari, H., Pattyn, F., Rußwurm, M., Kellenberger, B., Lhermitte, S., et al. (2024). Where the white continent is blue: Deep learning Locates Bare Ice in Antarctica. *Geophysical Research Letters*, *51*(3), e2023GL106285. https://doi.org/10.1029/2023GL106285

Touzeau, A., Landais, A., Stenni, B., Uemura, R., Fukui, K., Fujita, S., et al. (2016). Acquisition of isotopic composition for surface snow in East Antarctica and the links to climatic parameters. *The Cryosphere*, *10*(2), 837–852. https://doi.org/10.5194/tc-10-837-2016

Tripati, A. K., Sahany, S., Pittman, D., Eagle, R. A., Neelin, J. D., Mitchell, J. L., & Beaufort, L. (2014). Modern and glacial tropical snowlines controlled by sea surface temperature and atmospheric mixing. *Nature Geoscience*, *7*(3), 205–209. https://doi.org/10.1038/ngeo2082

Van Den Broeke, M. R., Winther, J.-G., Isaksson, E., Pinglot, J. F., Karlöf, L., Eiken, T., & Conrads, L. (1999). Climate variables along a traverse line in Dronning Maud Land, East Antarctica. *Journal of Glaciology*, *45*(150), 295–302. https://doi.org/10.3189/002214399793377266

Van der Hammen, T., & Hooghiemstra, H. (2000). Neogene and Quaternary history of vegetation, climate, and plant diversity in Amazonia. *Quaternary Science Reviews*, *19*(8), 725–742. https://doi.org/10.1016/s0277-3791(99)00024-4

Wang, Q., Fan, X., & Wang, M. (2014). Recent warming amplification over high elevation regions across the globe. *Climate Dynamics*, *43*(1–2), 87–101. https://doi.org/10.1007/s00382-013-1889-3

Whillans, I. M., & Cassidy, W. A. (1983). Catch a falling star: Meteorites and old ice. *Science*, *222*(4619), 55–57. https://doi.org/10.1126/science.222.4619.55

Williamson, S. N., Zdanowicz, C., Anslow, F. S., Clarke, G. K. C., Copland, L., Danby, R. K., et al. (2020). Evidence for elevation-dependent warming in the St. Elias Mountains, Yukon, Canada. *Journal of Climate*, *33*(8), 3253–3269. https://doi.org/10.1175/JCLI-D-19-0405.1

Wu, F., You, Q., Cai, Z., Sun, G., Normatov, I., & Shrestha, S. (2023). Significant elevation dependent warming over the Tibetan Plateau after removing longitude and latitude factors. *Atmospheric Research*, *284*, 106603. https://doi.org/10.1016/j.atmosres.2022.106603

Xie, A., Zhu, J., Qin, X., Wang, S., Xu, B., & Wang, Y. (2023). Surface warming from altitudinal and latitudinal amplification over Antarctica since the International Geophysical Year. *Scientific Reports*, *13*(1), 9536. https://doi.org/10.1038/s41598-023-35521-w

Yan, Y., Bender, M. L., Brook, E. J., Clifford, H. M., Kemeny, P. C., Kurbatov, A. V., et al. (2019). Two-million-year-old snapshots of atmospheric gases from Antarctic ice. *Nature*, *574*(7780), 663–666. https://doi.org/10.1038/s41586-019-1692-3

You, Q., Chen, D., Wu, F., Pepin, N., Cai, Z., Ahrens, B., et al. (2020). Elevation dependent warming over the Tibetan Plateau: Patterns, mechanisms and perspectives. *Earth-Science Reviews*, *210*, 103349. https://doi.org/10.1016/j.earscirev.2020.103349

Zekollari, H., Goderis, S., Debaille, V., Van Ginneken, M., Gattacceca, J., Timothy Jull, A. J., et al. (2019). Unravelling the high-altitude Nansen blue ice field meteorite trap (East Antarctica) and implications for regional palaeo-conditions. *Geochimica et Cosmochimica Acta*, *248*, 289–310. https://doi.org/10.1016/j.gca.2018.12.035

Zhu, J., Xie, A., Qin, X., Xu, B., & Wang, Y. (2024). Projection on elevation-dependent and latitude-dependent warming over Antarctica from CMIP6 under different socioeconomic scenarios. *Global and Planetary Change*, *232*, 104327. https://doi.org/10.1016/j.gloplacha.2023.104327